PHYSICAL REVIEW A **93**, 031801(R) (2016)

Periodic exploding dissipative solitons

Carlos Cartes and Orazio Descalzi*
Complex Systems Group, Facultad de Ingeniería y Ciencias Aplicadas, Universidad de los Andes, Avenida Monseñor Álvaro del Portillo 12455, Las Condes, Santiago, Chile
(Received 21 July 2014; published 4 March 2016)

We show the existence of periodic exploding dissipative solitons. These nonchaotic explosions appear when higher-order nonlinear and dispersive effects are added to the complex cubic-quintic Ginzburg-Landau equation modeling fiber soliton lasers. This counterintuitive phenomenon is the result of period-halving bifurcations leading to order (periodic explosions), followed by period-doubling bifurcations leading to chaos (chaotic explosions).

DOI: 10.1103/PhysRevA.93.031801

Soliton explosions were first experimentally observed in Kerr lens mode-locked Ti:sapphire lasers operating in a regime in which the soliton energy suffers dramatic changes [1]. A feature of the experimentally observed explosions is that they are similar but not identical; in fact, the time between explosions obeys a narrow distribution. Although the real system is not continuous, this dynamical behavior was predicted theoretically in a continuous model, namely, the complex cubic-quintic Ginzburg-Landau equation (CQGLE) [2,3].

Chaos in exploding solitons found by Soto-Crespo *et al.* [2] simulating the complex CQGLE in the anomalous dispersion regime has been further characterized theoretically in one and two spatial dimensions. In one spatial dimension a transition to exploding dissipative solitons (DS) mediated by pulses with rapid oscillations followed by pulses modulated with an additional small frequency has been reported [4]. This fact suggested an analog of the Ruelle-Takens route for spatially localized solutions [5]. In addition, it has been shown that the appearance of explosions has signatures of intermittency, for instance, the mean value of the time between explosions close to the criticality satisfies a power law [6]. In two spatial dimensions Soto-Crespo *et al.* showed first that pulsating beams can be transformed into exploding DS [7]. Recently, Cartes *et al.* have shown that the center of mass of asymmetric exploding DS undergoes a random walk (not necessarily Brownian motion) despite the deterministic character of the underlying model [8]. In addition, it has been found that noise can induce explosions for dissipative solitons [9].

In this Rapid Communication we show that besides chaotic exploding pulses there exist periodic nonchaotic explosions as a result of period-halving bifurcations leading to order (periodic explosions), followed by period-doubling bifurcations leading to chaos (chaotic explosions).

Very recently a new experiment leading to soliton explosions has been reported [10]. In contrast to the previous Kerr lens mode-locked solid-state laser [1] the new system consists of an all-normal-dispersion Yb-doped mode-locked fiber laser operating in a transition regime between stable and noise-like emission. The resulting experimental evidence has been successfully compared to realistic numerical simulations. The considered model for the complex electric field envelope $\tilde{\psi}(z,T)$ in a comoving frame reads [11]

$$\partial_{\tilde{z}}\tilde{\psi} - \frac{g(\tilde{z},P)}{2}\tilde{\psi} - i\sum_{k\geqslant 2}\frac{\beta_k}{k!}(i\partial_T)^k\tilde{\psi} = i\,\gamma\,(1+i\,\tau_{\text{shock}}\,\partial_T)\left(\tilde{\psi}\int_0^\infty R(T')|\tilde{\psi}(\tilde{z},T-T')|^2dT'\right), \tag{1}$$

where $g(\tilde{z},P)$ corresponds to the gain (or fiber loss), depending on the propagation distance $\tilde{z}$, and P, the pumping power. β_k stand for the dispersion coefficients and $\gamma = \omega_0 n_2(\omega_0)/[cA_{\text{eff}}(\omega_0)]$, where $n_2(\omega_0)$ is the nonlinear refractive index (or nonlinear Kerr parameter) and A_{eff} is the effective area of the fiber mode, evaluated at the carrier frequency ω_0. The time derivative term on the right-hand side of the above equation is associated with self-steepening and optical shock formation characterized by a time scale $\tau_{\text{shock}} \sim 1/\omega_0$. The response function $R(T)$ includes both instantaneous electronic and delayed Raman contributions.

Equation (1) is very general in the sense that it can be used for very short pulses. However, for pulses that are wide enough (~ 100 fs $= 0.1$ ps) we can make the following approximation [12]:

$$|\tilde{\psi}(\tilde{z},T-T')|^2 \approx |\tilde{\psi}(\tilde{z},T)|^2 - T'\partial_T|\tilde{\psi}(\tilde{z},T)|^2,$$

and Eq. (1) reduces to

$$\partial_{\tilde{z}}\tilde{\psi} - \frac{g(\tilde{z},P)}{2}\tilde{\psi} + i\,\frac{\beta_2}{2}\partial_T^2\tilde{\psi} - \frac{\beta_3}{6}\partial_T^3\tilde{\psi} = i\,\gamma\,|\tilde{\psi}|^2\tilde{\psi} - \frac{1}{\omega_0}\partial_T(|\tilde{\psi}|^2\tilde{\psi}) - iT_R\,\tilde{\psi}\,\partial_T(|\tilde{\psi}|^2), \tag{2}$$

where $\int_0^\infty R(t)dt = 1$ and $T_R \equiv \int_0^\infty tR(t)dt$.

The numerical results shown in Ref. [10] and based on Ref. [11] are ultimately related to the mode-locking details. In order to write an equation that can sustain dissipative pulses it is enough to assume a subcritical shape [13] for $\frac{g(\tilde{z},P)}{2}\tilde{\psi} \sim \mu_r\tilde{\psi} + \beta_r|\tilde{\psi}|^2\tilde{\psi} + \gamma_r|\tilde{\psi}|^4\tilde{\psi}$, and to consider a term $\sim D_r\partial_T^2\tilde{\psi}$, which might be interpreted as spectral filtering [1]. A large peak power associated with an optical pulse makes it (sometimes) necessary to replace γ by $\gamma_0(1-\gamma_1|\tilde{\psi}|^2)$, where γ_1 is a saturation parameter. Short pulses are dissipative solitons in the sense that they exist because of a complex balance between nonlinearity, dispersion, energy pump, and dissipation [14].

*Corresponding author: odescalzi@miuandes.cl

Taking into account the physical quantities P_0, L_D, and T_0, which correspond to the peak power, the dispersion length, and the width of the pulse, respectively, we can introduce the following dimensionless variables (ψ, z, τ):

$$\psi = \frac{\tilde{\psi}}{\sqrt{P_0}}, \quad z = \frac{\tilde{z}}{L_D}, \quad \tau = \frac{T}{T_0}, \tag{3}$$

where $P_0 \equiv \frac{|\beta_2|}{T_0^2 \gamma_0}$ and $L_D \equiv \frac{T_0^2}{|\beta_2|}$. Considering for silica fibers $|\beta_2| \sim 20$ ps^2/km, $T_0 = 0.1$ ps, $\lambda \sim 800$–1000 nm, $n_2 \sim 3.2 \times 10^{-20}$ m^2/W and a fiber with a core size of 1.7 μm in diameter we get $P_0 \sim 30$ W and $L_D \sim 0.5$ m.

By introducing the scaling (3) into Eq. (2) we obtain the dimensionless complex CQGLE including higher-order nonlinear and dispersive effects (HOE):

$$\begin{aligned} & i\,\partial_z \psi + \tfrac{1}{2}\partial_\tau^2 \psi + |\psi|^2 \psi - \nu\,|\psi|^4 \psi \\ & \quad = i\,\delta\,\psi + i\,\epsilon\,|\psi|^2 \psi + i\,\mu\,|\psi|^4 \psi + i\,\beta\,\partial_\tau^2 \psi + (\mathrm{HOE}), \\ & \quad (\mathrm{HOE}) \equiv i\,\delta_3\,\partial_\tau^3 \psi - i\,s\,\partial_\tau(|\psi|^2 \psi) + \tau_R\,\psi\,\partial_\tau(|\psi|^2), \end{aligned} \tag{4}$$

where $\nu \equiv \frac{\gamma_1 |\beta_2|}{T_0^2}$, $\delta \equiv \frac{\mu_r T_0^2}{|\beta_2|}$, $\epsilon \equiv \frac{\beta_r}{\gamma_0}$, $\mu \equiv \frac{\gamma_r |\beta_2|}{T_0^2 \gamma_0^2}$, $\beta \equiv \frac{D_r}{|\beta_2|}$, $\delta_3 \equiv \frac{\beta_3}{6 T_0 |\beta_2|}$, $s \equiv \frac{1}{\omega_0 T_0}$, $\tau_R \equiv \frac{T_R}{T_0}$, ν corresponds to a saturation higher-order term related to the intensity-dependent refractive index, δ accounts for the linear gain or loss, ϵ and μ account for the nonlinear gain or absorption, and β stands for the spectral filtering. The parameter ϵ is a suitable control parameter since it is related to the pumping power. The parameters δ_3, s, and τ_R represent, respectively, the effects of third-order dispersion (TOD), self-steepening (SST), and intrapulse Raman scattering (IRS). Figure 1 shows the evolution of periodic explosions with a duration about 1 ps. Figures 1(a) and 1(b) are qualitatively quite similar to experimental Figs. 2 and 5 in [10].

To get Eq. (4) we kept in mind many considerations: (a) The equation should incorporate the main physical ingredients at play in mode-locked lasers, in a distributed way; (b) dissipative quintic saturating terms are essential for the stability of the pulses; (c) the CQGLE is an extension of the Nonlinear Schroedinger (NLS) equation to higher order and dissipative terms; (d) it must have a continuous energy supply to the system (whenever the energy supply stops, solitons die; dissipative solitons have internal dynamics that make them analogous to biological objects); and (e) injection of energy must be related to the cubic term. Saturation comes with the quintic term. Figure 2(c) shows the dependence of the mean power of the exploding pulses as a function of ϵ. Mean power increases monotonically with ϵ but not necessarily linearly.

The left-hand side of Eq. (4) contain conservative terms. In fact, except for the quintic-order term we recover the NLS equation. While on the right-hand side the terms related to δ, ϵ, μ, and β are dissipative, the HOE includes only conservative terms.

Tian *et al.* found that nonlinear gradient terms result in dramatic changes in the soliton behavior leading to fixed-shape solitons [15]. Later, Latas *et al.* found that explosions can be controlled if these higher-order effects are properly conjugated two by two [16]. Recently, Cartes has shown that the transition

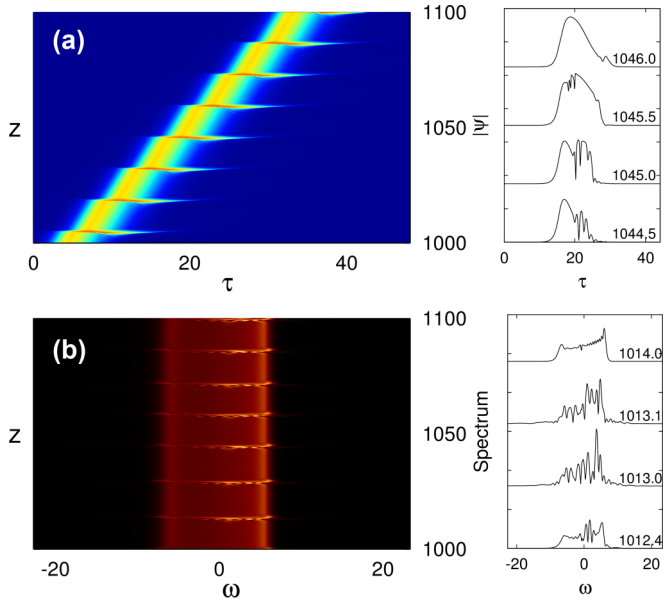

FIG. 1. Evolution of $|\psi|$ following the dimensionless complex CQGLE including higher-order nonlinear and dispersive effects [Eq. (4)]. (a) $|\psi|$ in a τ-z plot for periodic explosions and four representative snapshots of an explosion. (b) Evolution of the spectra corresponding to (a). $|\tilde{\psi}|^2 = 30$ W $\times\, |\psi|^2$. $\tau = 40$ corresponds to $T = 4$ ps and $z = 1100$ corresponds to $\tilde{z} = 550$ m. Parameters are $\delta = -0.1$, $\epsilon = 1.0188$, $\beta = 0.125$, $\mu = -0.1$, $\nu = 0.6$, $\delta_3 = 0.016$, $s = 0.009$, and $\tau_R = 0.032$.

between explosive and regular behavior can be characterized by a transcritical bifurcation controlled by the SST parameter [17]. Much earlier, the effect of nonlinear gradient terms on localized states in a complex cubic-quintic Ginzburg-Landau equation was studied by Brand *et al.* showing that these terms lead to asymmetries and reduction of the speed of the localized solutions [18,19].

It is well known that for relatively wide pulses ($T_0 \gg 1$ ps) the higher-order parameters (δ_3, s, τ_R) are negligible. However, for ultrashort pulses ($T_0 < 1$ ps) these parameters are no longer negligible and their influence increases as the pulse becomes shorter. Considering $T_0 \sim 0.1$ ps we can estimate $\tau_R \sim 0.03$ [12]. In addition we take relatively large values for δ_3 in order to test that explosions do not become destroyed because of the analogous behavior of the Cherenkov radiation [20].

For the simulations of Eq. (4) we keep all parameters fixed except for ϵ, which plays the role of a control parameter directly related to the pumping power: $\delta = -0.1$, $\beta = 0.125$, $\mu = -0.1$, $\nu = 0.6$, $\delta_3 = 0.016$, $s = 0.009$, and $\tau_R = 0.032$. In this Rapid Communication, simulations have been carried out using a box of size $N = 8192$ points, $dt = 0.01$ with $T = 81.92$, $dz = 0.004$, along a pseudospectral split-step method to compute the differential operator and a fourth-order Runge-Kutta scheme for the integration in z.

To study the influence of the third-order dispersion, self-steepening, and intrapulse Raman scattering on the exploding pulses we compute the energy $Q(z) = \int_0^T |\psi|^2 d\tau$ as it is presented in Fig. 2(a). In general this quantity has different values for its local maxima $Q_{\max}$, as shown in Fig. 2(b). In Fig. 3(a) we plot a logistic map for $Q_{\max}$ covering a small

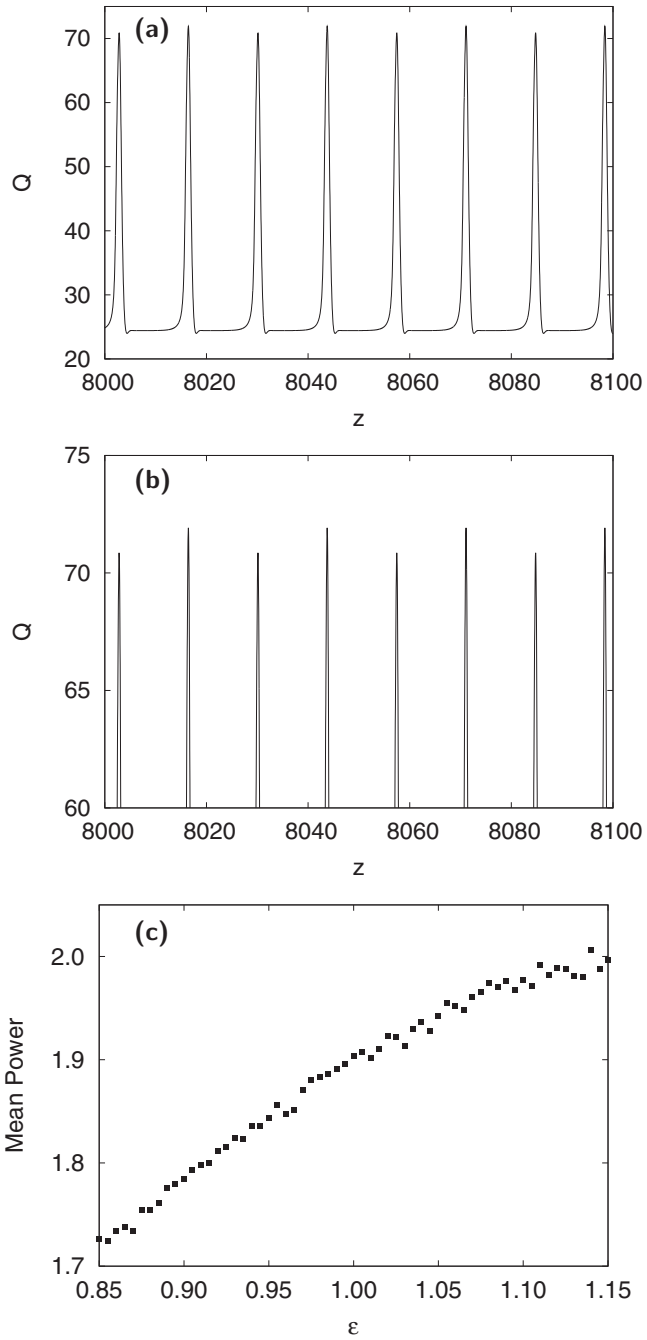

FIG. 2. (a) Energy $Q(z) = \int |\psi|^2 d\tau$ showing that explosions occur at intervals of length ~ 13.6. As the initial condition we used $u(t,0) = 1/\cosh(t)$. (b) A zoom of $Q(z)$ allows us to see two values of $Q_{\max}$ as it is plotted in Fig. 3. $z = 8000$ corresponds to $\tilde{z} = 4000$ m. $\int |\tilde{\psi}|^2 dT = P_0 T_0 Q(z)$, so that $Q_{\max} \sim 70$ corresponds to 0.2 nJ. Parameters are as in Fig. 1. (c) Dependance of the mean power of the exploding pulses as a function of ϵ. Mean power increases monotonically with ϵ but not necessarily linearly.

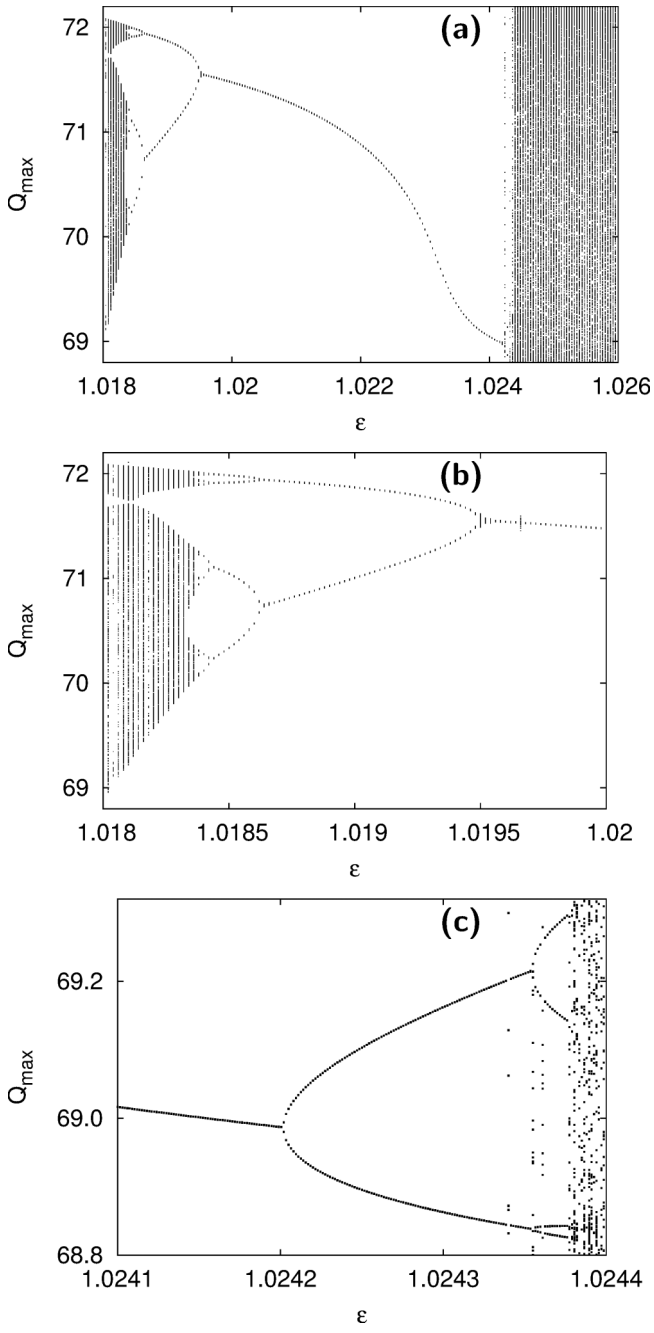

FIG. 3. (a) Logistic map for $Q_{\max}$ covering a small range of ϵ. (b) Zoom of the logistic map around $\epsilon = 1.019$ showing period-halving bifurcations leading to order. (c) Zoom of the logistic map around $\epsilon = 1.0243$ showing period-doubling bifurcations leading to chaos. Other parameters are as in Fig. 1.

range of ϵ. To avoid transients we recorded data after a propagation distance $z = 10^3$. For each value of ϵ we obtain, roughly, 10^3 explosions. One can see that a complex picture is obtained consistently with chaotic explosions. Chaotic explosions are already present without considering higher-order terms. However, looking at the logistics map in more detail we notice that there are windows corresponding to nonchaotic behavior. This situation is generic in the sense that we observe this fact for a large range of the control parameters (not shown in Fig. 3) and for different values of TOD, SST, and IRS parameters. Figures 3(b) and 3(c) present a zoom emphasizing period-halving and period-doubling bifurcations leading to order and chaos, respectively.

As a second characterization of periodic explosions we plot in Fig. 4 the peak of the amplitude $|\psi|_{\text{peak}}$ versus energy Q

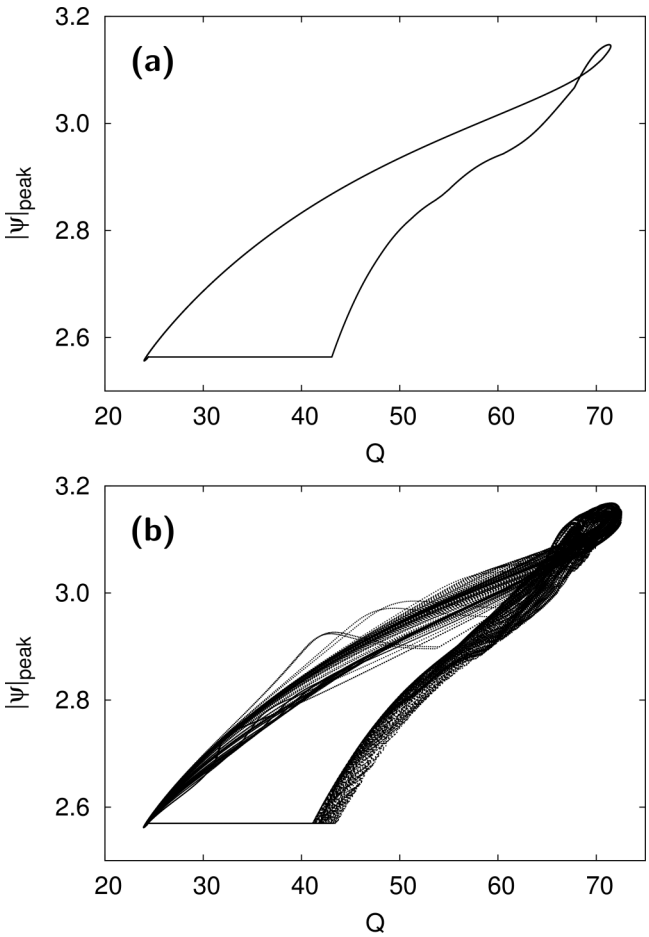

FIG. 4. (a) Peak of the amplitude $|\psi|_{\text{peak}}$ versus energy for (nonchaotic) periodic explosions for $\epsilon = 1.02$. (b) Peak of the amplitude $|\psi|_{\text{peak}}$ versus energy for chaotic explosions for $\epsilon = 1.025$. Other parameters are as in Fig. 1.

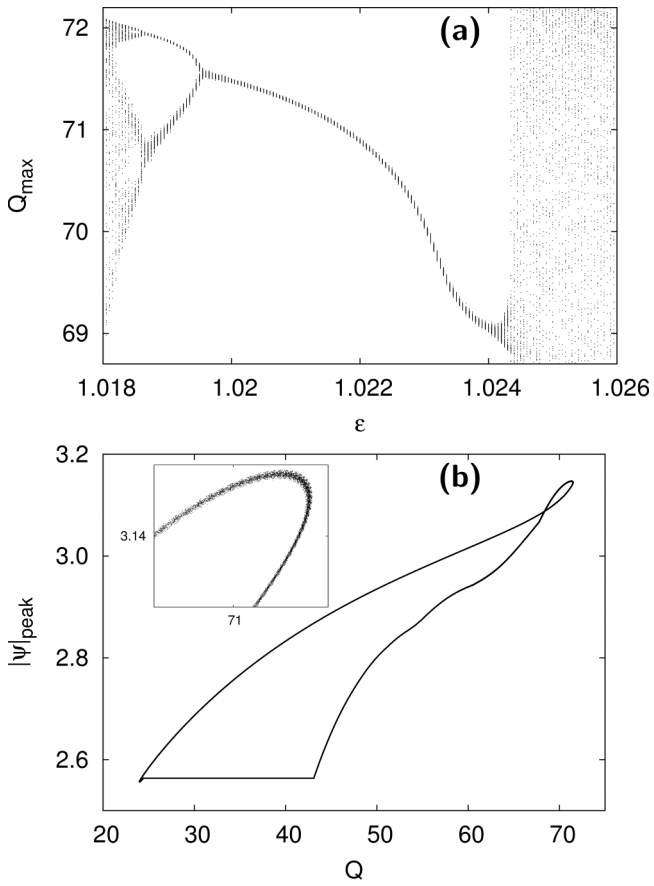

FIG. 5. (a) Noisy version of Fig. 2(a). (b) Noisy version of Fig. 3(a). Other parameters are as in Fig. 1 and $\eta = 10^{-7}$. Inset emphasizes the stochastic character of the depicted curve.

for periodic explosions [Fig. 4(a)] and for chaotic explosions [Fig. 4(b)]. We found that for periodic explosions, after a period ζ, $|\psi(t,z_0+\zeta)|$ coincides exactly with $|\psi(t,z_0)|$ even on a logarithmic scale. We also studied the persistence of the periodic behavior for very long propagation distances, to be sure that this behavior is not a very slow transient.

To study the effect of noise on periodic explosions we add additive noise $\eta\,\xi$ to Eq. (4), where η is the noise strength. The stochastic force $\xi(\tau,z)$ denotes white noise with the properties $\langle\xi\rangle = 0$, $\langle\xi(\tau,z)\,\xi(\tau',z')\rangle = 0$, and $\langle\xi(\tau,z)\,\xi^*(\tau',z')\rangle = 2\delta(\tau-\tau')\delta(z-z')$, where ξ^* denotes the complex conjugate of ξ. Figure 5(a) represents the noisy version of Fig. 3(a), and Fig. 5(b) the noisy version of Fig. 4(a).

We found that a small amount of noise, on the order of $\eta = 10^{-6}$ or less, still preserves the periodic character of explosions, only adding a slight stochastic behavior that is shown in Fig. 5(b) and its inset. These stochastic-periodic explosions are qualitatively different compared to their chaotic counterparts, as can be seen by comparing Figs. 4(b) and 5(b).

In summary we have shown the existence of periodic nonchaotic explosions in the cubic-quintic Ginzburg-Landau equation considering higher-order nonlinear and dispersive effects. This counterintuitive phenomenon is the result of period-halving bifurcations leading to order (periodic explosions), followed by period-doubling bifurcations leading to chaos (chaotic explosions). Natural candidates to study these predictions are Kerr lens mode-locked Ti:sapphire lasers and Yb-doped mode-locked fiber lasers. The complex behavior shown here is low-dimensional, as can be seen from

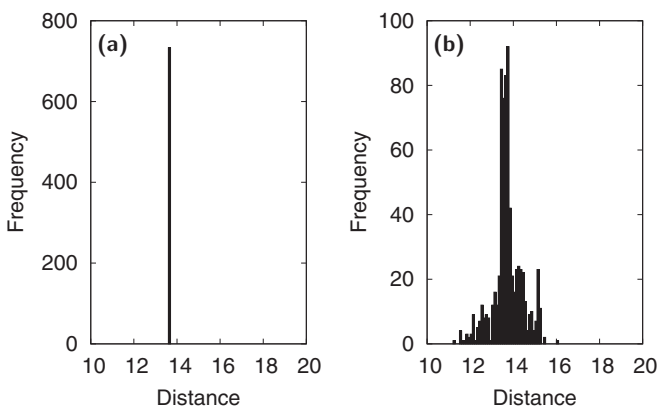

FIG. 6. Histograms of distances between explosions. (a) Distance between periodic explosions is fixed ($\epsilon = 1.020$). (b) Distances between nonperiodic explosions exhibit dispersion ($\epsilon = 1.025$). Other parameters are as in Fig. 1.

Refs. [4–6], and structurally unstable, that is, small changes in the parameter ϵ might lead to qualitatively different behaviors (order $\rightarrow$ chaos or, in other words, from periodic exploding solitons to chaotic exploding solitons or vice versa). The goal of this paper is precisely to show this phenomenon. Reaching this kind of precision in an experiment could be difficult, but a practical method to distinguish between periodic and nonperiodic explosions is to record a histogram of distances between soliton explosions, as shown in Fig. 6. We think it is relevant to stress the importance of accurate simulations, which through parameter exploration one can find interesting chaotic phenomena that are very difficult to directly find in experiments without previous knowledge.

We thank Jaime Cisternas and Jaime Anguita for valuable comments and we acknowledge the support of FONDECYT (Chile, Grant No. 1140139), and the Research Office, Universidad de los Andes, Chile.

[1] S. T. Cundiff, J. M. Soto-Crespo, and N. Akhmediev, Phys. Rev. Lett. **88**, 073903 (2002).
[2] J. M. Soto-Crespo, N. Akhmediev, and A. Ankiewicz, Phys. Rev. Lett. **85**, 2937 (2000).
[3] N. Akhmediev, J. M. Soto-Crespo, and G. Town, Phys. Rev. E **63**, 056602 (2001).
[4] O. Descalzi and H. R. Brand, Phys. Rev. E **82**, 026203 (2010).
[5] O. Descalzi, C. Cartes, J. Cisternas, and H. R. Brand, Phys. Rev. E **83**, 056214 (2011).
[6] J. Cisternas and O. Descalzi, Phys. Rev. E **88**, 022903 (2013).
[7] J. M. Soto-Crespo, N. Akhmediev, N. Devine, and C. Mejia-Cortes, Opt. Express **16**, 15388 (2008).
[8] C. Cartes, J. Cisternas, O. Descalzi, and H. R. Brand, Phys. Rev. Lett. **109**, 178303 (2012).
[9] C. Cartes, O. Descalzi, and H. R. Brand, Phys. Rev. E **85**, 015205(R) (2012).
[10] A. F. J. Runge, N. G. R. Broderick, and M. Erkintalo, Optica **2**, 36 (2015).
[11] A. F. J. Runge, C. Aguergaray, R. Provo, M. Erkintalo, and N. G. R. Broderick, Opt. Fiber Technol. **20**, 657 (2014).
[12] G. P. Agrawal, *Nonlinear Fiber Optics* (Academic, New York, 2013).
[13] O. Thual and S. Fauve, J. Phys. (Paris) **49**, 1829 (1988).
[14] Ph. Grelu and N. Akhmediev, Nat. Photon. **6**, 84 (2012).
[15] H. P. Tian, Z. H. Li, J. P. Tian, G. S. Zhou, and J. Zi, Appl. Phys. B **78**, 199 (2004).
[16] S. C. V. Latas and M. F. S. Ferreira, Opt. Lett. **35**, 1771 (2010); **36**, 3085 (2011); **37**, 3897 (2012).
[17] C. Cartes and O. Descalzi, Eur. Phys. J. ST **223**, 91 (2014).
[18] R. J. Deissler and H. R. Brand, Phys. Lett. A **146**, 252 (1990).
[19] R. J. Deissler and H. R. Brand, Phys. Rev. Lett. **81**, 3856 (1998).
[20] N. Akhmediev and M. Karlsson, Phys. Rev. A **51**, 2602 (1995).